



1 **Biodiversity and trophic ecology of hydrothermal vent fauna associated with**
2 **tubeworm assemblages on the Juan de Fuca Ridge**

3

4 Yann Lelièvre^{1,2*}, Jozée Sarrazin¹, Julien Marticorena¹, Gauthier Schaal³, Thomas Day¹, Pierre
5 Legendre², Stéphane Hourdez⁴, Marjolaine Matabos¹

6

7 ¹Ifremer, Centre de Bretagne, REM/EEP, Laboratoire Environnement Profond, 29280
8 Plouzané, France

9 ²Département de sciences biologiques, Université de Montréal, C.P. 6128, succursale Centre-
10 ville, Montréal, Québec, H3C 3J7, Canada

11 ³Laboratoire des Sciences de l'Environnement Marin (LEMAR), UMR 6539
12 CNRS/UBO/IRD/Ifremer, BP 70, 29280, Plouzané, France

13 ⁴Sorbonne Universités, UPMC Univ. Paris 06, CNRS UMR 7144, Adaptation et Diversité en
14 Milieu Marin, Station Biologique de Roscoff, 29688 Roscoff, France

15

16 **Corresponding author**

17 Lelièvre Yann

18 (1) Département de sciences biologiques, Université de Montréal, C.P. 6128, succursale
19 Centre-ville, Montréal, Québec, H3C 3J7, Canada; (2) Ifremer, Centre de Bretagne, REM/EEP,
20 Laboratoire Environnement Profond, 29280 Plouzané, France.

21

22 Telephone number in Canada: +1 514 343 7591

23 Email address: yann.lelievre@ifremer.fr



24 **Abstract**

25 Hydrothermal vent sites along the Juan de Fuca Ridge in the north-east Pacific host dense
26 populations of *Ridgeia piscesae* tubeworms that promote habitat heterogeneity and local
27 diversity. A detailed description of the biodiversity and community structure is needed to
28 help understand the ecological processes that underlie the distribution and dynamics of
29 deep-sea vent communities. Here, we assessed the composition, abundance, diversity and
30 trophic structure of six tubeworm assemblages, corresponding to different successional
31 stages, collected on the Grotto hydrothermal edifice (Main Endeavour, Juan de Fuca Ridge)
32 at 2196 m depth. Including *R. piscesae*, a total of 36 macrofaunal taxa were identified to the
33 species level. Although polychaetes made up the most diverse taxon, faunal densities were
34 dominated by gastropods. Most tubeworm aggregations were numerically dominated by the
35 polychaete *Amphisamytha carldarei* and gastropods *Lepetodrilus fucensis* and *Depressigyra*
36 *globulus*. The highest diversities were found in mature tubeworm aggregations,
37 characterized by fairly long tubes. The high biomass of grazers and the high resource
38 partitioning at small scale illustrates the importance of the diversity of free-living microbial
39 communities in the maintenance of the food web. Although symbiont-bearing invertebrates
40 *R. piscesae* represented a large part of the total biomass, the absence of specialized
41 predators on this potential food source suggests that its primary role lies in community
42 structuring. Vent food webs did not appear to be organized through predator-prey
43 relationships. For example, although trophic structure complexity increased with ecological
44 successional stages, showing a higher number of predators in the last stages, the food web
45 structure itself did not change across assemblages. We suggest that environmental gradients
46 provided by the biogenic structure of tubeworm bushes generate a multitude of ecological
47 niches and contribute to the partitioning of nutritional resources, releasing communities
48 from competition pressure for resources, thus allowing species co-existence.

49

50 *Keywords:* Juan de Fuca Ridge; hydrothermal vents; *Ridgeia piscesae*; community structure;
51 *diversity; stable isotopes; food webs.*



52 **1. Introduction**

53 Deep-sea hydrothermal vents have developed along mid-ocean ridges and back-arc
54 spreading centres, which are characterized by strong volcanic and tectonic activity. The
55 resulting hydrothermal fluid fosters dense communities of highly specialized fauna that
56 colonize the steep physical and chemical gradients created by the mixing of hot vent fluids
57 with cold seawater. These communities are distributed according to species' physiological
58 tolerance (Childress and Fisher, 1992; Luther et al., 2001), resource availability (De
59 Busserolles et al., 2009; Levesque et al., 2003) and biotic interactions (Lenihan et al., 2008;
60 Micheli et al., 2002; Mullineaux et al., 2000, 2003). Although the fauna are highly dissimilar
61 between oceanic basins (Bachraty et al., 2009; Moalic et al., 2011), hydrothermal
62 communities throughout the world share some ecological similarities including a food web
63 based on chemosynthesis (Childress and Fisher, 1992), low species diversity compared with
64 adjacent deep-sea and coastal benthic communities (Van Dover and Trask, 2000; Tunnicliffe,
65 1991), high levels of endemism (Ramirez-Llodra et al., 2007), and elevated biomass
66 associated with the presence of large invertebrate species.

67

68 The high spatial heterogeneity of environmental conditions in vent ecosystems is amplified
69 by stochastic or periodic temporal variation in hydrothermal activity, influencing the
70 composition (Sarrazin et al., 1999), structure (Marcus et al., 2009; Sarrazin et al., 1997;
71 Tsurumi and Tunnicliffe, 2001) and dynamics (Lelièvre et al., 2017; Nedoncelle et al., 2013,
72 2015; Sarrazin et al., 2014) of faunal communities. In addition, the complexity of vent
73 habitats is increased by engineer species, whose presence strongly contributes to the
74 modification of the physical (temperature, hydrodynamics processes) and chemical
75 (hydrogen sulfide, methane, oxygen, metals and other reduced chemicals) properties of the
76 environment either by creating three-dimensional biogenic structures (autogenic species) or
77 through their biological activity (allogenic species) (Jones et al., 1994, 1997). Habitat
78 provisioning and modification by engineer species increases the number of potential
79 ecological niches and, consequently, influences species distribution and contributes to the
80 increase in local diversity (Dreyer et al., 2005; Govenar and Fisher, 2007; Urcuyo et al.,
81 2003). Engineer species promote local diversity through various ecological mechanisms
82 (Bergquist et al., 2003), providing secondary substratum for colonization, a refuge from



83 predation and unfavourable abiotic conditions or important food sources that enhance the
84 development of macro- and meiofaunal communities (Dreyer et al., 2005; Galkin and
85 Goroslavskaya, 2010; Gollner et al., 2006; Govenar et al., 2005, 2002; Govenar and Fisher,
86 2007; Turnipseed et al., 2003; Zekely et al., 2006).

87

88 Hydrothermal vent food webs are mainly based on local microbial chemosynthesis (Childress
89 and Fisher, 1992), performed by free-living or/and symbiotic chemoautotrophic
90 microorganisms that utilize the chemical energy released in the oxidation of reduced
91 chemicals species (e.g. H₂S, CH₄) present in the hydrothermal fluids (Childress and Fisher,
92 1992). Several electron donors (e.g. H₂, H₂S, CH₄, NH₄⁺, etc.) and electron acceptors (e.g. O₂,
93 NO₃⁻, SO₄²⁻, etc.) can be used by these microorganisms as energy sources, converting
94 inorganic carbon (e.g. CO₂) into simple carbohydrates (Fisher et al., 2007). Chemosynthetic
95 primary production is exported to the upper trophic levels through direct ingestion (primary
96 consumers), or through the presence of intra- or extracellular symbiosis. Upper trophic
97 levels (secondary consumers) are represented by local predators and scavengers feeding on
98 primary consumers and by abyssal species attracted by the profusion of food. Although
99 behavioural observations and stomach content analyses remain limited in these remote
100 deep-sea habitats, stable isotope analyses are widely used to study faunal trophic
101 interactions in these environments (Conway et al., 1994). The emergence of isotopic
102 methods has opened new perspectives in the understanding of food-web functioning and
103 the organization of species diversity within hydrothermal ecosystems around the globe
104 (Bergquist et al., 2007; De Busserolles et al., 2009; Van Dover, 2002; Erickson et al., 2009;
105 Gaudron et al., 2012; Levesque et al., 2006; Levin et al., 2009; Limén et al., 2007; Portail et
106 al., 2016; Soto, 2009; Sweetman et al., 2013). The carbon isotope composition ($\delta^{13}\text{C}$) is an
107 indicator of the food assimilated and remains relatively constant during trophic transfers
108 ($\pm 1\%$). The kinetics of enzymes involved in the biosynthetic pathways of autotrophic
109 organisms influence the carbon isotope ratio ($^{13}\text{C}/^{12}\text{C}$), allowing the discrimination between
110 the sources fuelling the community (Conway et al., 1994; Van Dover and Fry, 1989). Nitrogen
111 isotope composition ($\delta^{15}\text{N}$) provides information on trophic levels (Michener and Lajtha,
112 2008) and becomes enriched in heavy isotopes at a rate of $\pm 3.4\%$ at each trophic level. At
113 the community scale, $\delta^{13}\text{C}$ and $\delta^{15}\text{N}$ signatures of all species in the ecosystem are used to
114 retrace carbon and nitrogen fluxes along the trophic network and, therefore, to reconstitute



115 the food web (Levin and Michener, 2002). Despite the relatively low diversity of the deep-
116 sea community, ample evidence suggests that the deep-sea hydrothermal food-web
117 structure is complex (Bergquist et al., 2007; Portail et al., 2016) including many trophic guilds
118 (Bergquist et al., 2007; De Busserolles et al., 2009) and multiple sources of primary
119 production (Van Dover and Fry, 1994).

120

121 Active hydrothermal vents on the Juan de Fuca Ridge (north-east Pacific) are colonized by
122 populations of the siboglinid polychaete *Ridgeia piscesae* (Urcuyo et al., 2003) forming dense
123 faunal assemblages in areas of high to low fluid flux activity. Diverse heterotrophic faunal
124 species inhabit these tubeworm bushes, with a dominance of polychaete and gastropod
125 species (Bergquist et al., 2007; Govenar et al., 2002; Marcus et al., 2009; Tsurumi and
126 Tunnicliffe, 2001, 2003). To date, few studies have described the communities associated
127 with the *R. piscesae* tubeworm assemblage of the Main Endeavour vent field, either in terms
128 of diversity (Bergquist et al., 2007; Sarrazin et al., 1997) or trophic ecology (Bergquist et al.,
129 2007). Six distinct faunal assemblages exhibiting patchy distributions have been identified on
130 the Smoke & Mirrors hydrothermal edifice, and represent different successional stages
131 (Sarrazin et al., 1997). Assemblages I and II are characterized by pioneer *Paralvinella*
132 *palmiformis* polychaete species that colonize new unstable high-temperature surfaces and
133 whose biological activity tends to stabilize the substratum (Juniper et al., 1992; Sarrazin et
134 al., 1997). Assemblage III is marked by dense aggregations of *P. palmiformis* and the
135 colonization of high densities of gastropods *Lepetodrilus fucensis*, *Depressigyra globulus* and
136 *Provanna variabilis* (Sarrazin et al., 1997). Assemblage IV is characterized by the growth of *R.*
137 *piscesae*, leading to assemblage V associated with a more complex physical structure and
138 consequently with an increase in local diversity, density and biomass (Bergquist et al., 2003;
139 Sarrazin et al., 1997; Tsurumi and Tunnicliffe, 2003). Finally, assemblage VI characterizes a
140 senescent phase in which *R. piscesae* gradually dies and its associated species disappear,
141 with a dominance of filamentous bacteria and detritivores (Sarrazin et al., 1997). A
142 successional model proposes that the transition between the first two assemblages is mostly
143 driven by biotic interactions, and those between the other assemblages are principally
144 initiated by modifications in hydrothermal activity (Sarrazin et al., 1997). Within a single
145 assemblage of *R. piscesae* tubeworm from diffuse flow vent environments of Easter Island



146 (Main Endeavour, Juan de Fuca Ridge), Bergquist *et al.* (2007) reported that tubeworm-
147 generated habitats supported a diverse community, with a complex local food web.

148

149 Since 2011, a camera installed on the *Ocean Networks Canada* cabled observatory has been
150 recording high-resolution imagery of a *R. piscesae* tubeworm assemblage and its associated
151 fauna on the active Grotto hydrothermal edifice (Main Endeavour, Juan de Fuca Ridge). The
152 processing of this data provided new insights on the influence of astronomic and
153 atmospheric forcing on vent faunal dynamics (Lelièvre *et al.*, 2017), but thorough knowledge
154 of the faunal communities observed by the camera is still needed to understand and
155 interpret the temporal patterns and their underlying mechanisms. However, although video
156 imagery is useful for investigating the spatial distribution of communities (Cuvelier *et al.*,
157 2011; Sarrazin *et al.*, 1997), species behaviour (Grelon *et al.*, 2006; Matabos *et al.*, 2015) and
158 temporal dynamics of a sub-set of the species (Cuvelier *et al.*, 2014; Lelièvre *et al.*, 2017),
159 direct sampling is an essential and complementary approach for determining faunal
160 composition, abundance and species diversity and functioning (Cuvelier *et al.*, 2012). In this
161 context, the objectives of the present study were: (i) to identify the composition and
162 structure of six faunal assemblages associated with *R. piscesae* tubeworm bushes on the
163 Grotto hydrothermal edifice, specifically with respect to density, biomass and species
164 diversity; (ii) to characterize the trophic structure of these biological communities and (iii) to
165 assess how diversity and trophic relationship vary over the different successional stages.

166

167 **2. Materials and Methods**

168 **2.1. Geological setting**

169 The Juan de Fuca Ridge (JdFR) (Fig. 1a) is an intermediate spreading-rate ridge between the
170 Pacific and Juan de Fuca plates in the north-east Pacific Ocean. The Endeavour Segment
171 (47°57'N, 129°06'W) (Fig. 1b) constitutes a ~ 90 km long section of the JdFR, bounded to the
172 north by the Middle Valley site and to the south by the Cobb Segment. It is characterized by
173 a 500–1000 m wide axial valley whose walls reach up to 200 m in height (Delaney *et al.*,
174 1992). The five major vent fields – Sasquatch, Salty Dawg, High Rise, Main Endeavour (MEF)
175 and Mothra – found on the Endeavour axial valley are separated by 2–3 km.

176



177 The MEF (Fig. 1c) is the most intense and active of the five hydrothermal fields, with the
178 presence of high-temperature (370-390°C), actively venting sulfide edifices and diffuse low-
179 temperature (10-25°C) venting areas (Delaney et al., 1992; Kelley et al., 2012). Within the
180 MEF, Grotto (47°56.958'N, 129°5.899'W, Fig. 1d) is an active hydrothermal sulfide vent
181 cluster (15 m long by 10 m wide by 10 m high) located at 2196 m depth that forms an open
182 cove to the north. This edifice is characterized by high short-term variation in heat flux, but a
183 relative stability in years with low seismic activity (Xu et al., 2014). Like many other MEF
184 hydrothermal edifices, the site is largely colonized by dense assemblages of *R. piscesae*
185 (Polychaeta, Siboglinidae) with their associated fauna (Sarrazin et al., 1997).

186

187 **2.2. Faunal assemblage sampling**

188 Sampling took place during the ONC oceanographic cruises *Wiring the Abyss 2015 and 2016*
189 from 25 August to 14 September 2015 on the R/V *Thomas G. Thompson*, and from 10 May to
190 29 May 2016 on the E/V *Nautilus*, respectively. Using the remotely operated vehicles (ROVs)
191 *Jason* and *Hercules*, three assemblages of *R. piscesae* tubeworms and their associated fauna
192 were sampled each year at different locations on the Grotto hydrothermal edifice (n=6; S1 to
193 S6, Fig. 2). For each sample, a checkerboard of 7 x 7 mm squares was first placed on each
194 tubeworm assemblage to estimate the surface area. Then, the first suction sample was
195 taken to recover the mobile fauna, followed by collection of tubeworms and their associated
196 fauna, which were placed in a “bio-box” using the ROV’s mechanical arm. A final suction
197 sample on the bare surface was performed to recover the remaining fauna. The final
198 sampled surface was filmed with the ROV camera to estimate its surface using imagery (see
199 protocol in Sarrazin *et al.* 1997 (Sarrazin et al., 1997)).

200

201 **2.3. Sample processing**

202 *2.3.1. Sample processing and identification*

203 On board, all faunal samples were washed over stacked sieves (250 µm, 63 µm and 20 µm
204 mesh sizes). Macrofaunal specimens (>250 µm) were preserved in 96 % ethanol and
205 meiofauna (<63 µm) in 10 % seawater formalin. In the laboratory, bushes of *R. piscesae* were
206 thoroughly disassembled and each tube was washed and sieved a second time. All
207 associated macrofaunal organisms were sorted, counted and identified to the lowest



208 possible taxonomic level. Specimens whose identification was unclear were sent to experts
209 for identification and/or description. When available, trophic guilds from the literature
210 (symbiont host, bacterivore, scavenger/detritivore or predator) were assigned to each vent
211 species. For species with unknown diets, the assignment was based on trophic guilds
212 identified from closely related species (within the same family).

213

214 *2.3.2 Habitat complexity and biomass*

215 For each tubeworm assemblage, the density measured in number of individuals per square
216 meter (ind m^{-2}) was calculated. In addition to the surface they occupy, *R. piscesae* tubes
217 create a three-dimensional (3D) structure for other vent animals to colonize. An estimation
218 of the volume of each assemblage provided a proxy for habitat complexity. For this, in each
219 sample, 10 % of the tubeworm tubes were randomly selected and measured. Assuming that
220 the tubes are erected vertically, sampling volume was estimated by multiplying the mean
221 tube length by the sampled surface area. Final densities are therefore expressed per m^3 to
222 account for this 3D space. Biomass estimates were obtained for a random sample of 3 to 10
223 individuals of each species. The total dry mass (DM) of each species corresponds to the mass
224 obtained after drying each individual at 80°C for 48 h; the ash-free dry mass (AFDM) was
225 obtained after combustion in a muffle furnace at 500°C for 6 h. Absolute biomass of each
226 species was calculated by multiplying the relative biomass by the abundance of each species.
227

228 *2.3.3. Stable isotope processing*

229 Sample preparation for stable isotope analyses was specimen size-dependent. For large
230 specimens, muscle tissue was dissected and used for stable isotope analyses. In the case of
231 intermediate-size specimens, the gut content was removed. For small taxa, entire individuals
232 were analysed or pooled to reach the minimum required mass for isotopic analysis. Samples
233 were freeze-dried and ground into a homogeneous powder using a ball mill or agate mortar.
234 About 1.3-1.4 mg of the powder was precisely measured in tin capsules for isotope analysis.
235 For species containing carbonates (i.e. gastropods, ostracods, amphipods, etc.), individuals
236 were acidified to remove inorganic carbon. Acidification was carried out by the addition of
237 0.1 M HCl. The sample was then dried at 60°C for 24 h under a fume extractor to evaporate
238 the acid. Five replicates per species were analysed. Carbon and nitrogen isotope ratios were



239 determined using a Thermo Scientific FLASH EA 2000 elemental analyser coupled with a
240 Thermo Scientific Delta V Plus isotope ratio mass spectrometer. Values are expressed in δ
241 (‰) notation relative to Vienna Pee Dee Belemnite and atmospheric N_2 as international
242 standards for carbon and nitrogen, respectively, according to the formula: $\delta^{13}C$ or $\delta^{15}N =$
243 $[(R_{\text{sample}}/R_{\text{standard}})-1] \times 10^3$ (in ‰) where R is $^{13}C/^{12}C$ or $^{15}N/^{14}N$. Analytical precision based on
244 repeated measurements of the same sample was below 0.3‰ for both $\delta^{13}C$ and $\delta^{15}N$.

245

246 2.4. Statistical analyses

247 In the present study, *R. piscesae* was regarded as a habitat builder and thus discarded from
248 the statistical analyses. Species-effort curves were computed for each faunal sample
249 collected to assess the robustness of the sampling effort. Local diversity (i.e. α diversity) was
250 estimated for each tubeworm assemblage from several complementary indices (Gray, 2000)
251 using the vegan package in R (Oksanen et al., 2017): species richness (S), exponential
252 Shannon entropy (D), Simpson's $(1-\lambda')$ indices of species diversity and Pielou's evenness
253 index (J').

254

255 3. Results

256 3.1. Species-effort curves, tubeworm complexity and diversity

257 The rarefaction curves (Fig. 3) showed that, overall, the collected samples (S1 to S6) gave a
258 fairly good representation of the species diversity on the Grotto hydrothermal edifice. In
259 2015, sample S2 (24 taxa, excluding *R. piscesae*) and S3 (31 taxa) rarefaction curves seemed
260 to reach a plateau. S1 cumulated a total of 28 macrofaunal taxa. The samples from year
261 2016 exhibited lower species richness and did not reach an asymptote. Samples S4 and S5
262 had a macrofaunal species richness of 19 taxa, while only 14 taxa were found in sample S6
263 (Fig. 3).

264

265 The volumes of the samples were used as an approximate measure of habitat complexity of
266 the 3D structures of the *R. piscesae* assemblages. Samples S1 and S3 showed similar
267 patterns, with sampling surfaces of 12.36 and 11.92 dm² and mean tube lengths of
268 17.24 ± 6.38 and 17.89 ± 5.69 cm, respectively (Table 1). Therefore, S1 and S3 were
269 characterized by a similar degree of complexity, with a volume of 21.31 and 21.33 dm³.



270 Sample S2 displayed a sampling area of less than half of that of S1 and S3 (6.33 dm²) and a
271 mean tube length of 8.16 ± 2.14 cm with an estimated resulting volume of 5.16 dm³.
272 Samples S4 to S6 were substantially smaller than S1, S2 and S3, with a sampling surface
273 between 1.22 and 1.59 dm². *R. piscesae* tubes were short in samples S4 and S5 leading to a
274 sampling volume of 0.7 and 0.86 dm³ respectively (Table 1). Sample S6 displayed tube
275 lengths similar to S2 leading to a sampling volume of 1.02 dm³ (Table 1).

276

277 Alpha diversity measures showed that S3 displayed the highest diversity (Shannon $D = 6.053$;
278 $1-\lambda' = 0.778$), slightly greater than S2 ($D = 5.398$; $1-\lambda' = 0.749$) and S1 ($D = 5.377$; $1-\lambda' = 0.728$)
279 (Table 1). The lowest diversity values were observed in S5 ($D = 4.348$; $1-\lambda' = 0.697$), S6
280 ($D = 3.998$; $1-\lambda' = 0.633$) and S4 ($D = 2.605$; $1-\lambda' = 0.550$). The S2 and S3 samples showed a
281 more even distribution (J') of individuals among taxa than the other assemblages. In
282 contrast, S4 had the lowest evenness ($J' = 0.325$) (Table 1). Species richness was significantly
283 correlated with *R. piscesae* tube length ($R^2_{\text{adj}} = 0.60$, $p\text{-value} = 0.042$).

284

285 3.2. Composition and structure of Grotto vent communities

286 The species lists and abundances for each sample collected within the Grotto hydrothermal
287 edifice are provided in Table 2. A total of 148 005 individuals representing 35 macrofaunal
288 taxonomic groups were identified in the six *R. piscesae* assemblages (S1 to S6) sampled on
289 the Grotto edifice. Overall, gastropods (5 taxa) and polychaetes (19 taxa) respectively
290 accounted for 61.51 ± 16.9 % and 29.06 ± 13.06 % of the total macrofaunal abundance. The
291 numerically most abundant species were the gastropods *L. fucensis* and *D. globulus* as well
292 as the polychaete *Amphisamytha carldarei* representing respectively 33.95 ± 7.58 %,
293 24.54 ± 15.68 % and 15.08 ± 13.57 % of the total abundance. The highest macrofaunal
294 densities were observed in samples S4 ($19\,364\,286$ ind m⁻³), S5 ($7\,461\,628$ ind m⁻³), S2
295 ($5\,196\,318$ ind m⁻³) and S3 ($3\,143\,241$ ind m⁻³), whereas S6 and S1 had the lowest densities
296 with $1\,607\,843$ ind m⁻³ and $1\,523\,932$ ind m⁻³, respectively. The foundation species *R.*
297 *piscesae* represented a large part of the total biomass, with a mean of 69.3 ± 15.7 % of the
298 total biomass, followed by the gastropods *L. fucensis* (14.96 ± 4.05 %) and *D. globulus* ($6.76 \pm$
299 8.34 %). A high percentage (30 %) of the species were only found in 1 or 2 samples.



300

301 More specifically, S1 was dominated by gastropod species such as *L. fucensis* (617 785 ind m⁻³;
302 ³; 12.48 % of total biomass), *D. globulus* (156 265 ind m⁻³; 1.12 % of total biomass) and *P.*
303 *variabilis* (27 452 ind m⁻³; 2.25 % of total biomass) (Table 2). High densities contrasted with
304 low biomass were also observed for the ampharetid polychaete *A. carldarei* and the syllid
305 polychaete *Sphaerosyllis ridgensis*. S2 was also dominated by *L. fucensis*, *D. globulus* and *A.*
306 *carldarei*, with, however, a high proportion of ostracods *Euphilomedes climax* (475 388
307 ind m⁻³; 0.10 % of total biomass) (Table 2). S3 was largely dominated by *A. carldarei*
308 (1 073 511 ind m⁻³; 1.84 % of total biomass) and, to a lesser extent, was almost equally
309 dominated by *L. fucensis* (702 438 ind m⁻³; 11.53 % of total biomass) and *D. globulus*
310 (619 784 ind m⁻³; 2.86 % of total biomass). Polychaetes were also dominant, with the
311 presence of *S. ridgensis* (52 414 ind m⁻³; <0.001 % of total biomass), the dorvilleid
312 *Ophryotrocha globopalpata* (40 319 ind m⁻³; <0.001 % of total biomass) and the maldanid
313 *Nicomache venticola* (7079 ind m⁻³; 1.09 % of total biomass). There were high densities of *P.*
314 *variabilis* (138 678 ind m⁻³; 6.78 % of total biomass), the solenogaster *Helicoradomenia juani*
315 (172 011 ind m⁻³; 0.14 % of total biomass), the acarida *Copidognathus papillatus*
316 (150 633 ind m⁻³; <0.001 % of total biomass), the ostracod *Xylocythere sp. nov.*
317 (82 419 ind m⁻³; <0.001 % of total biomass) and the pycnogonid *Sericosura verенаe* (22 644
318 ind m⁻³; 0.84 % of total biomass) (Table 2). S4 was dominated by *L. fucensis* (7 700 000 ind m⁻³;
319 ³; 19.43 % of total biomass) and *D. globulus* (9 195 714 ind m⁻³; 13.02 % of total biomass)
320 and, to a lesser extent, by the alvinellid polychaete *P. palmiformis* (591 429 ind m⁻³; 6.78 %
321 of total biomass) (Table 2). S5 was also dominated by *L. fucensis* and *D. globulus*, followed by
322 *E. climax* (624 419 ind m⁻³; <0.001 % of total biomass) and *P. variabilis* (594 186 ind m⁻³; 10 %
323 of total biomass) (Table 2). Finally, S6 was also dominated *L. fucensis* and *D. globulus* and, to
324 a lesser extent, by *A. carldarei* (86 275 ind m⁻³; 0.07 % of total biomass) and the alvinellid
325 polychaete *Paralvinella pandorae* (63 725 ind m⁻³; <0.001 % of total biomass) (Table 2).

326

327 **3.4. $\delta^{13}\text{C}$ and $\delta^{15}\text{N}$ isotopic composition**

328 $\delta^{13}\text{C}$ values of the vent fauna ranged from -33.4 to -11.8 ‰ among the different samples
329 (Fig. 4). More specifically, $\delta^{13}\text{C}$ values ranged from -33.4 to -13.5 ‰ for S1, from -33.4 to
330 -15.4 ‰ for S2 and from -32.4 to -14.7 ‰ for S3. Samples from S4, S5 and S6 displayed
331 slightly narrower $\delta^{13}\text{C}$ ranges, varying from -30.3 to -12.5 ‰, from -31.3 to -14.8 ‰ and



332 from -32.3 to -11.8 ‰, respectively; most species were enriched in ^{13}C relative to the S1, S2
333 and S3 samples (Fig. 4). Overall, the gastropod *P. variabilis* (species #2) was the most
334 depleted in ^{13}C with values around -32.2 ‰ (± 1.2 ‰). In contrast, *R. piscesae* siboglinids
335 (species #1) showed the highest $\delta^{13}\text{C}$ values, with constant values around -14.7 ‰ (\pm
336 1.0 ‰). The range of $\delta^{15}\text{N}$ values in faunal assemblages varied between -8.5 and 9.4 ‰ (Fig.
337 4). More specifically, S1 values ranged from 0.3 to 8.4 ‰, S2 from 0.4 to 9.2 ‰, S3 from -2.7
338 to 8.3 ‰, S4 from -1.3 to 8.7 ‰, S5 from -1.1 to 6.4 ‰ and S6 from -8.5 to 9.4 ‰ (Fig. 4).
339 Overall, 15 species showed a $\delta^{15}\text{N} > 5$ ‰ in S1, S2 and S3 assemblages but only 4 species
340 were over 5‰ in $\delta^{15}\text{N}$ in S4, S5 and S6. In contrast to their $\delta^{13}\text{C}$ values, *P. variabilis* and *R.*
341 *piscesae* displayed similar and relatively stable $\delta^{15}\text{N}$ values among samples with 0.3 ‰
342 (± 0.8 ‰) and 1.5 ‰ (± 1.1 ‰), respectively.

343

344 3.5. Biomass distribution in the Grotto trophic network

345 The projection of the species isotopic ratios weighted by biomass is useful for estimating the
346 relative contributions of the different trophic pathways within the vent assemblages (Fig. 5).
347 In our study, there were similar patterns of biomass distribution in the six sampled
348 assemblages. In all samples, the engineer polychaete *R. piscesae* (species #1) represented
349 the highest biomass (69.3 ± 16 %). It was considered to be a structuring species of our vent
350 ecosystem and was not included in the following biomass distribution analysis. With a
351 biomass ranging from 78.9 to 95.8 % (89.6 ± 6.8 %), gastropods seemed to play an important
352 role in the trophic food web of communities associated with the siboglinid tubeworms. The
353 gastropod biomass was dominated by *L. fucensis* (species #4), which accounted for 31.5 to
354 82.8 % (55.8 ± 18.3 %) of the total biomass. In addition to *L. fucensis*, the gastropods *D.*
355 *globulus* (species #3), *P. variabilis* (species #2) and *Buccinum thermophilum* (species #5)
356 showed relatively high biomass within the different samples, ranging from 5.6 to 36.6 %
357 (16.5 ± 13.8 %), 0.6 to 26.3 % (10.9 ± 9.8 %) and 0 to 16.1 % (6.4 ± 6.8 %), respectively (Fig.
358 5). However, in some assemblages, other species also significantly contributed to the total
359 biomass. For example, in S3, the polychaete *A. carldarei* (species #7) contributed
360 substantially (7.2 %) to the total biomass. Similarly, in S4, the polychaete *P. palmiformis*
361 (species #13) contributed to 16.4 % of the total biomass. Our results also show that the
362 biomass declined from the bacterivore to the predator guilds in the Grotto trophic network.

363



364 4. Discussion

365 4.1. Communities and diversity

366 Hydrothermal ecosystems of the north-east Pacific are dominated by dense populations of
367 tubeworms *R. piscesae*. In this study, a total of 36 macrofaunal taxonomic groups (including
368 *R. piscesae*) were found in the six tubeworm assemblages sampled on the Grotto edifice,
369 which is consistent with previous community knowledge in the region (Bergquist et al.,
370 2007). In this study, macrofaunal species richness was slightly lower than that observed at
371 the Easter Island hydrothermal site on the Main Endeavour Field, where a total of 39 species
372 had been identified in a single *R. piscesae* bush (Bergquist et al., 2007). Another study also
373 reported the presence of 39 macrofaunal species in 25 collections from the Axial Segment
374 (JdFR), but lower values have been reported on other segments, with 24 species in 7
375 collections from the Cleft Segment (JdFR) and 19 species in 2 collections from the CoAxial
376 Segment (JdFR) (Tsurumi and Tunnicliffe, 2003). These levels of diversity are lower than that
377 found in *Riftia pachyptila* bushes on the East Pacific Rise, where species richness in 8
378 collections reached 46 taxa (Govenar et al., 2005). Macrofaunal diversity was also lower than
379 those obtained in engineer mussel beds from Lucky Strike on the Mid-Atlantic Ridge, with 41
380 taxa identified (Sarrazin et al., 2015), or from the northern and southern East Pacific Rise,
381 with richnesses of 61 and 57 taxa, respectively (Van Dover, 2003). Faunal dissimilarities
382 between worldwide hydrothermal ecosystems may be closely related to the geological
383 context (ridge, back-arc basins), history of species colonization, connectivity to neighbouring
384 basins, presence of geographic barriers (transform faults, hydrodynamic processes, depths,
385 etc.), stability of hydrothermal activity, age of the vent system and inter-site distances (Van
386 Dover et al., 2002). Discrepancies in sampling effort may also account for variation between
387 sites and regions.

388

389 *R. piscesae* tubeworm assemblages sampled on the Grotto edifice were characterized by the
390 dominance of a few species (e.g. *L. fucensis*, *D. globulus*, *A. carldarei*), a pattern that has also
391 been reported from other hydrothermal sites of the world oceans: Mid-Atlantic Ridge
392 (Cuvelier et al., 2011; Sarrazin et al., 2015), East Pacific Rise (Govenar et al., 2005), JdFR
393 (Sarrazin and Juniper, 1999; Tsurumi and Tunnicliffe, 2001) and the southern East Pacific Rise
394 (Matabos et al., 2008). Polychaetes were the most diverse taxa, representing half of the



395 macrofaunal species richness (19 taxa). Similar results have been reported within *R. piscesae*
396 bushes on Easter Island, with the identification of 23 polychaete species (Bergquist et al.,
397 2007). Although the dominant species were similar among samples, variation between
398 samples involved mainly the relative abundance of the few dominant species and the
399 identity of the rare species. These variations may result from differences in sampling
400 strategy. The areas sampled in 2016 were smaller than in 2015 and a problem with the
401 sampling boxes may have led to the loss of some individuals. Variation in species richness
402 and diversity among samples may also depend on the presence of environmental gradients,
403 created by the mixing between ambient seawater and hydrothermal effluents (Sarrazin et
404 al., 1999). Unfortunately, no environmental data were recorded with our samples. However,
405 physical and chemical conditions are known to change along the ecological succession
406 gradient on the MEF from newly opened habitat characterized by high temperature and
407 sulfide concentrations, colonized by the sulfide worm *Paralvinella sulfincola*, to mature
408 communities in low diffuse venting areas characterised by low temperatures and sulfide
409 concentrations and colonized by long skinny *R. piscesae* tubeworms (Sarrazin et al., 1997).
410 Tubeworm assemblages S1 and S3 were visually recognized as type V low-flow assemblages
411 (Sarrazin et al., 1997), characterized by a mature phase of *R. piscesae* bush development and
412 a high level of complexity. This assessment was confirmed by the length of the collected
413 tubes (17 cm on average). Both assemblages showed the highest species richness, diversity
414 and most complex trophic network, illustrating the strong influence of engineer species and
415 the importance of biogenic structure in the diversification and persistence of the local
416 resident fauna. By increasing the number of micro-niches available for vent species, the 3D
417 structure of *R. piscesae* bushes helps to increase the environmental heterogeneity and
418 thereby promotes species richness and diversity at community scales (Jones et al., 1997;
419 Tsurumi and Tunnicliffe, 2003). As mentioned by several authors (Bergquist et al., 2003;
420 Govenar et al., 2002; Tsurumi and Tunnicliffe, 2003), various ecological mechanisms may
421 explain the influence of *R. piscesae* tubeworms on local diversity: new habitats generated by
422 tubeworm bushes provide (i) a substratum for attachment and colonization; (ii) interstitial
423 spaces among intertwined tubes, increasing habitat gradients and therefore the number of
424 ecological niches; (iii) a refuge to avoid predators and to reduce the physiological stress
425 related to abiotic conditions and (iv) a control on the transport of hydrothermal vent flow
426 and nutritional resource availability. Assemblages S2 and S5, also identified as type V low-



427 flow assemblages (Sarrazin et al., 1997), presented shorter tube lengths than S1 and S3,
428 which might explain the lower species richness in these two samples. Polychaete densities
429 on Grotto were dominated by the ampharetid *A. carldarei* (89.9 ± 2.8 %, not including S4 and
430 S6). High densities in *R. piscesae* assemblages may be related to the specificity of this family
431 with high ecological tolerance to environmental conditions and, therefore, to their ability to
432 take advantage of a wide range of ecological niches (McHugh and Tunnicliffe, 1994). Similar
433 to *L. fucensis*, *A. carldarei* is characterized by early maturity and high fecundity, contributing
434 to the success of this species in vent habitats (McHugh and Tunnicliffe, 1994). The
435 dominance of gastropods *L. fucensis* and *D. globulus* as well as the relatively high presence
436 of the *Paralvinella* polychaete species in samples S4 and S6 suggest that they belong to
437 lower succession levels, corresponding to transitory states between types III and IV
438 assemblages (Sarrazin et al., 1997). The latter two samples were characterized by low
439 species richness and diversities. We hypothesize that the numerical dominance of
440 gastropods negatively affected species diversity by monopolizing space and nutritional
441 resources, therefore reducing the settlement of other vent species. The grazing of new
442 recruits may also limit species diversity. Successional community dynamics leading to the
443 development of tubeworm assemblages may thus result in the diversification of the habitats
444 and of the species therein, and by a complexification of the trophic network, as suggested by
445 Sarrazin *et al.* (2002) (Sarrazin et al., 2002).

446

447 **4.2. Trophic structure of tubeworm assemblages**

448 The *R. piscesae* tubeworm assemblages of the Grotto hydrothermal edifice harbour a
449 relatively diverse heterotrophic fauna. The isotopic analyses conducted on the most
450 dominant vent species within the bushes revealed a high degree of resemblance in trophic
451 structure among the six faunal assemblages.

452

453 Hydrothermal food webs are generally based on two main energetic pathways: the transfer
454 of energy from symbionts to host invertebrates and the consumption of free-living microbial
455 production (Bergquist et al., 2007). In the present study, the contrasting isotope
456 compositions of the gastropods *P. variabilis*, *L. fucensis* and the polychaete *R. piscesae*
457 suggest three large pools of isotopically distinct, symbiotic and/or free-living microbial
458 production available to primary consumers. The high $\delta^{13}\text{C}$ values of *R. piscesae* were



459 associated with chemosynthetic endosymbiosis linked to thiotrophic symbionts (Hügler and
460 Sievert, 2011). *R. piscesae* contributed to 86 % of the assemblage biomass, but few species
461 displayed similar $\delta^{13}\text{C}$ values, suggesting that species deriving their food sources from
462 siboglinid tubeworms are rare. Similar observations, where engineer species contribute to
463 the community more as a habitat than as a food source, have been reported in *R. piscesae*
464 tubeworm bushes from the Easter Island vent site (Bergquist et al., 2007) or in
465 *Bathymodiolus azoricus* mussel bed communities on the Tour Eiffel hydrothermal edifice
466 (Lucky Strike, Mid-Atlantic Ridge) (De Busserolles et al., 2009). The low degree of
467 exploitation of this large biomass and potential food resource suggests that *R. piscesae* plays
468 a primarily structuring role in vent ecosystems rather than a trophic role. Nevertheless, the
469 $\delta^{13}\text{C}$ and $\delta^{15}\text{N}$ values of polynoid predators *Branchinotogluma tunnicliffae* and
470 *Lepidonotopodium piscesae* were consistent with a diet including *R. piscesae* tubeworms.
471 Predation on tubeworms was confirmed by a video sequence from the ecological
472 observatory module TEMPO-mini, deployed on the Grotto hydrothermal edifice (ONC
473 observatory; Video S1). The ^{13}C -depleted stable isotope compositions of *P. variabilis* suggest
474 a possible symbiosis with chemoautotrophic bacteria or reliance on feeding on a very
475 specific free-living microbial community that depends on a ^{13}C -depleted carbon source
476 (Bergquist et al., 2007). To date, no study has reported the presence of chemoautotrophic
477 symbionts in *P. variabilis*, but symbioses have been described for other species from the
478 Provannidae family (Windoffer and Giere, 1997). With an intermediate $\delta^{13}\text{C}$ composition
479 between *R. piscesae* and *P. variabilis*, *L. fucensis* gastropods seem to represent a major
480 energetic pathway in these vent communities. In addition, the different food webs obtained
481 in this study revealed that most vent species display an isotope composition centred on *L.*
482 *fucensis*. The position of *L. fucensis* at the base of the food web probably reflects direct
483 access to suspended food particles from hydrothermal fluid emissions. The high densities
484 and large biomass of *L. fucensis* in tubeworm bushes, and its capacity to exploit different
485 food sources through different feeding modes (Bates, 2007), may exert a high pressure on
486 the availability of nutritional resources and, therefore, lead to an important role in
487 structuring vent communities. Whenever present, the *Paralvinella* species, which are non-
488 selective deposit-feeders, also displayed low $\delta^{15}\text{N}$ values, suggesting a role at the base of the
489 food web. The stable isotope composition of *Paralvinella* species was much more variable



490 among samples than for the former three species, suggesting a possible variability in
491 nutrient sources.

492

493 Like in many vent food webs (Van Dover and Fry, 1994; Levesque et al., 2005; Limén et al.,
494 2007), Grotto primary consumers were dominated by grazers and deposit feeders. The high
495 diversity, densities and biomass of bacterivores emphasize the importance of free-living
496 bacteria in the establishment and maintenance of the structure of the vent food web
497 (Bergquist et al., 2007). This guild was mainly represented by the gastropods *P. variabilis*, *D.*
498 *globulus* and *L. fucensis* and by the polychaetes *P. sulfincola*, *P. palmiformis*, *P. pandorae* and
499 *Paralvinella dela*. The polychaete *P. sulfincola* can feed directly on microbial biofilms on the
500 substratum around its tube opening (Grelon et al., 2006), which may explain the low $\delta^{15}\text{N}$
501 values of alvinellids in the present study. Like *Paralvinella grasslei* and *Paralvinella*
502 *bactericola* at vent sites of the Guaymas Basin (Portail et al., 2016), the alvinellid species
503 found at Grotto had comparable $\delta^{13}\text{C}$ values but different $\delta^{15}\text{N}$ signatures. The species *P.*
504 *pandorae* showed a depleted $\delta^{15}\text{N}$ signature relative to other alvinellid species. A previous
505 study of spatial isotope variability among three sympatric alvinellid species, *P. palmiformis*,
506 *P. sulfincola* and *P. pandorae* on the JdFR reported that this difference in $\delta^{15}\text{N}$ isotope
507 composition was closely related to food-source partitioning and/or to spatial segregation
508 (Levesque et al., 2003). The comparatively small size of *P. pandorae* (Lelièvre Y., personal
509 observation) compared with other alvinellid species may be the result of interspecific
510 competition for food resources and/or a diet based on an isotopically distinct microbial
511 source. The wide range of $\delta^{13}\text{C}$ signatures in bacterivores, coupled with the high interspecific
512 variability in the isotopic space, suggest a large, diversified microbial pool in the
513 hydrothermal ecosystem and high variability in isotope ratios in dominant microbial taxa.
514 Detritivore/scavenger species were observed at an intermediate trophic level, between the
515 bacterivore and predator feeding guilds. This guild was represented by a low number of
516 species including the gastropod *B. thermophilum*, the ampharetid *A. carldarei* and the
517 orbiiniid *Berkeleyia sp. nov.* The predator-feeding guild was represented by the highest $\delta^{15}\text{N}$
518 values. High predator diversity was found in our vent assemblages, and was associated with
519 a wide range of $\delta^{13}\text{C}$ values, covering the isotopic spectrum of lower trophic level consumers
520 (i.e. bacterivores as well as scavengers/detritivores). This guild of predators appears to be
521 dominated by polychaetes, which tend to show the highest $\delta^{15}\text{N}$ values. Whenever present,



522 the syllid *Sphaerosyllis ridgensis*, the polynoid *Levensteiniella kincaidi* and the hesionid
523 *Hesiospina sp. nov.* displayed the highest $\delta^{15}\text{N}$ values, suggesting that they play the role of
524 top predators in the benthic food web. Similarly, the solenogaster *Helicoradomenia juani*
525 consistently displayed higher $\delta^{15}\text{N}$ values than other molluscs, indicating a predator trophic
526 position. Except for the polynoid *L. kincaidi*, whose isotopic variability seemed to reveal a
527 nutrition based on highly diversified food resources, stable isotope analyses conducted on
528 predators revealed narrow ranges of $\delta^{13}\text{C}$ and $\delta^{15}\text{N}$ values at the species scale, suggesting
529 the dominance of specialist-feeding strategies, as was the case for the bacterivores. An
530 accurate assessment of food sources and a description of the meiofaunal communities
531 would be necessary to better understand the functioning of these chemosynthetic
532 communities and their trophic structures.

533

534 **4.3. Ecological niche partitioning**

535 Vent species on the Grotto hydrothermal edifice exhibit high isotopic heterogeneity that
536 reflects the complexity of vent ecological networks. The distribution of species in the bi-
537 dimensional isotopic space depends on their diets, environmental conditions and biotic
538 interactions, which together define the concept of species ecological niche (Newsome et al.,
539 2007) or the realized species trophic niche (Bearhop et al., 2004). Here, the fact that most of
540 the isotopic space was occupied by isotopically distinct species shows that the available food
541 resources are partitioned within the community. Although the $\delta^{15}\text{N}$ variability among
542 primary consumers did hinder our inference of trophic levels based on nitrogen isotopes,
543 these communities are unlikely to host more than three trophic levels, given the overall $\delta^{15}\text{N}$
544 ranges. Moreover, although predators were quite diverse, they only represented a minor
545 part of the biomass, suggesting that Grotto vent communities are mostly driven by bottom-
546 up processes. Food webs of chemosynthetic ecosystems – such as hydrothermal vents and
547 cold seeps – do not appear to be structured along predator-prey relationships, but rather
548 through weak trophic relationships among co-occurring species (Levesque et al., 2006;
549 Portail et al., 2016). Habitat and/or trophic partitioning are important structuring processes
550 at the community scale (Levesque et al., 2003; Levin et al., 2013; Portail et al., 2016). Our
551 results corroborate with those from Axial Volcano in the JdFR (Levesque et al., 2006) and the
552 Guaymas basin (Portail et al., 2016), where habitat heterogeneity induces spatial partitioning
553 of trophic niches, leading to a spatial segregation of species and species coexistence



554 (Levesque et al., 2006). Although the observed isotope variability (standard deviations) in
555 Grotto vent species suggests the occurrence of both trophic specialists and generalists
556 within the assemblages, the majority of vent species exhibited low standard deviations,
557 suggesting a predominantly specialist feeding behaviour. As already shown in previous
558 studies of vent sites with alvinellids (Levesque et al., 2003) and sulfidic sediments at
559 methane seeps with dorvilleid polychaetes (Levin et al., 2013) in the north-east Pacific, food
560 partitioning may occur between different species of the same or closely related taxonomic
561 family, allowing species coexistence through occupation of distinct trophic niches. For
562 example, hydrothermal vent gastropods were numerically dominant in all *R. piscesae* bushes
563 collected on the Grotto edifice and their isotope compositions were fairly diverse.
564 Gastropods exhibit great diversity in feeding strategies, and as a result they are found in a
565 wide variety of niches where they exploit many food sources (Bates et al., 2005; Bates,
566 2007). The isotope composition of *P. variabilis* indicated low $\delta^{13}\text{C}$ and $\delta^{15}\text{N}$ values. *L. fucensis*
567 gastropods had higher $\delta^{13}\text{C}$ and $\delta^{15}\text{N}$ values than *P. variabilis* but a similar range of $\delta^{13}\text{C}$ as
568 *Clypeosectus curvus* and *D. globulus*. However, these latter two species occupy an upper
569 position in the trophic structure of their communities. The great ecological success of *L.*
570 *fucensis* in vent habitats may be attributed to a combination of several characteristics. First,
571 this species is characterized by a broad trophic plasticity that includes: (i) grazing on
572 siboglinid tubeworms and hard substrata (Fretter, 1988), (ii) active suspension feeding
573 (Bates, 2007) and (iii) harbouring filamentous bacterial epibionts in its gills, which – via
574 endocytosis – may contribute to the animal's nutritional requirements (Bates, 2007; Fox et
575 al., 2002). In addition, the early maturity, high fecundity, and continuous gamete production
576 of *L. fucensis* may help to maintain the large populations on the edifice (Kelly and Metaxas,
577 2007). Stacking behaviour near fluid emissions also suggests that *L. fucensis* is an important
578 competitor for space and food in the community (Tsurumi and Tunnicliffe, 2003). *L. elevatus*,
579 the ecological equivalent of *L. fucensis* on the East Pacific Rise, is a prey for the vent zoarcid
580 fish *Thermarces cerberus*; the reduced limpet population promotes the successful
581 settlement and growth of sessile benthic invertebrates such as tubeworms (Micheli et al.,
582 2002; Sancho et al., 2005). The potential absence of an equivalent predator for *L. fucensis*
583 and the biological characteristics detailed above may explain its ecological success on the
584 north-east Pacific vent sites. In contrast, the nutrition of *D. globulus* is based on the grazing
585 of organic matter only (Warén and Bouchet, 1989). However, its small size allows it to



586 exploit interstitial spaces that are not available to larger fauna (Bates et al., 2005). Finally, *P.*
587 *variabilis* was relatively less abundant than the other two species, but appeared to exploit a
588 different thermal niche than *L. fucensis* and *D. globulus* (Bates et al., 2005). On the other
589 hand, the isotope composition of *B. thermophilum* clearly differentiates that species from
590 the other gastropods with higher $\delta^{13}\text{C}$ signatures. Differences in the diets of co-occurring
591 species may contribute to the high abundance – such as *L. fucensis* and *D. globulus* – and
592 diversity of vent gastropods through niche partitioning (Govenar et al., 2015).

593

594 Habitat specialization among co-occurring vent species may drive differences in their diets
595 (Govenar et al., 2015), facilitating species coexistence in heterogeneous habitats such as
596 hydrothermal ecosystems. We hypothesized that in vent engineering ecosystems, food webs
597 display a spatial structure at small scale with regard to the microhabitats generated by the
598 3D architecture of biogenic structures that promote high interspecific trophic segregation.
599 The spatial segregation of trophic niches by environmental gradients limits the occurrence of
600 biotic interactions such as predation and competition for resources between species sharing
601 a common spatial niche (Levesque et al., 2006). Vent food webs may therefore be structured
602 through the interplay between the availability and diversity of food sources and the abiotic
603 and biotic conditions structuring species distribution.

604

605 **5. Conclusion**

606 This study provides the first characterization of the macrofaunal diversity and trophic
607 ecology of vent communities associated with *R. piscesae* tubeworm assemblages on the
608 Grotto hydrothermal edifice. Like many vent structures (Cuvelier et al., 2011; Sarrazin et al.,
609 1997), the Grotto hydrothermal edifice is inhabited by a mosaic of habitats and faunal
610 assemblages that may represent different successional stages characterized by different
611 abiotic conditions. Our results show that the development of *R. piscesae* tubeworms
612 introduces complexity and heterogeneity in the hydrothermal environments and exerts a
613 strong influence on ecosystem properties. The 3D structure of these tubeworms enhances
614 community diversity and thereby increases the potential trophic interactions between vent
615 species in the food web. Environmental gradients provided by the interstitial spacing of
616 intertwined tubeworms generate a multitude of ecological niches and contribute to the
617 partitioning of nutritional resources, leading to the species coexistence. Habitat



618 modifications incurred by *R. piscesae* bushes may thus directly stimulate the development of
619 complex food webs. Thorough knowledge of hydrothermal biodiversity and ecological
620 functioning of these remote ecosystems is necessary to determine their uniqueness and
621 contribute to the protection and conservation of this natural heritage.

622

623 **Author's contributions**

624 M.M., J.S. and P.L. designed and supervised the research project. Y.L., J.M., T.D. and S.H.:
625 data acquisition and analyses. Y.L., M.M., J.S., G.S. and P.L. conceived the ideas and
626 contributed to the interpretation of the results. All authors contributed to the writing
627 process and revised the manuscript.

628

629 **Competing interests**

630 The authors declare that they have no conflict of interest.

631

632 **Acknowledgments**

633 The authors thank the captains and crews of the R/V *Thomas G. Thompson* and E/V *Nautilus*,
634 the staffs of Ocean Networks Canada and ROV *Jason* and *Hercules* pilots during the "*Ocean*
635 *Networks Canada Wiring the Abyss*" cruises in 2015 and 2016. We thank also Kim Juniper
636 and the government of Canada for work permits to study in Canadian waters (XR281, 2015;
637 XR267, 2016). Thanks also to Pauline Chauvet for faunal sampling during the ONC 2016
638 cruise. This research was supported by a NSERC research grant to P.L. and IFREMER funds. It
639 was also funded by the *Laboratoire d'Excellence LabexMER* (ANR-10-LABX-19) and co-funded
640 by a grant from the French government under the *Investissements d'Avenir* programme. We
641 are also grateful to the numerous taxonomists around the world who contributed to species
642 identification and to the laboratory *Centre de Recherche sur les Interactions Bassins Versants*
643 *- Écosystèmes Aquatiques* (RIVE) at the Université du Québec à Trois-Rivières (Canada) for
644 the isotope sample processing. The manuscript was professionally edited by Carolyn Engel-
645 Gautier. This paper is part of the Ph.D. thesis of Y.L. carried out under joint supervision
646 between Université de Montréal and Université de Bretagne Occidentale/Ifremer.

647



648 **References**

- 649 Bachraty, C., Legendre, P. and Desbruyères, D.: Biogeographic relationships among deep-sea
650 hydrothermal vent faunas at global scale, *Deep. Res. Part I Oceanogr. Res. Pap.*, 56(8), 1371–
651 1378, 2009.
- 652 Bates, A., Tunnicliffe, V. and Lee, R. W.: Role of thermal conditions in habitat selection by
653 hydrothermal vent gastropods, *Mar. Ecol. Prog. Ser.*, 305, 1–15, 2005.
- 654 Bates, A. E.: Feeding strategy, morphological specialisation and presence of bacterial
655 epibionts in lepetodrilid gastropods from hydrothermal vents, *Mar. Ecol. Prog. Ser.*, 347,
656 87–99, 2007.
- 657 Bearhop, S., Adams, C. E., Waldron, S., Fuller, R. A. and Macleod, H.: Determining trophic
658 niche width: a novel approach using stable isotope analysis, *J. Anim. Ecol.*, 73(5), 1007–1012,
659 2004.
- 660 Bergquist, D., Ward, T., Cordes, E., McNelis, T., Howlett, S., Kosoff, R., Hourdez, S., Carney, R.
661 and Fisher, C.: Community structure of vestimentiferan-generated habitat islands from Gulf
662 of Mexico cold seeps, *J. Exp. Mar. Bio. Ecol.*, 289(2), 197–222, 2003.
- 663 Bergquist, D. C., Eckner, J. T., Urcuyo, I. A., Cordes, E. E., Hourdez, S., Macko, S. A. and Fisher,
664 C. R.: Using stable isotopes and quantitative community characteristics to determine a local
665 hydrothermal vent food web, *Mar. Ecol. Prog. Ser.*, 330(1), 49–65, 2007.
- 666 De Busserolles, F., Sarrazin, J., Gauthier, O., Gélinas, Y., Fabri, M.-C., Sarradin, P.-M. and
667 Desbruyères, D.: Are spatial variations in the diets of hydrothermal fauna linked to local
668 environmental conditions?, *Deep. Res. Part II Top. Stud. Oceanogr.*, 56(19–20), 1649–1664,
669 2009.
- 670 Childress, J. J. and Fisher, C. R.: The biology of hydrothermal vent animals: physiology,
671 biochemistry, and autotrophic symbioses, *Oceanogr. Mar. Biol. Annu. Rev.*, 30, 337–441,
672 1992.
- 673 Conway, N. M., Kennicutt, M. C. and Van Dover, C. L.: Stable isotopes in the study of marine
674 chemosynthetic-based ecosystems, in *Stable isotopes in ecology and environmental science*,
675 pp. 158–186., 1994.
- 676 Couvelier, D., Sarradin, P.-M., Sarrazin, J., Colaço, A., Copley, J. T., Desbruyères, D., Glover, A.
677 G., Serrao Santos, R. and Tyler, P. A.: Hydrothermal faunal assemblages and habitat
678 characterisation at the Eiffel Tower edifice (Lucky Strike, Mid-Atlantic Ridge), *Mar. Ecol.*,



- 679 32(2), 243–255, 2011.
- 680 Cuvelier, D., De Busserolles, F., Lavaud, R., Floc’h, E., Fabri, M.-C., Sarradin, P. M. and
681 Sarrazin, J.: Biological data extraction from imagery - How far can we go? A case study from
682 the Mid-Atlantic Ridge, *Mar. Environ. Res.*, 82, 15–27, 2012.
- 683 Cuvelier, D., Legendre, P., Laes, A., Sarradin, P.-M. and Sarrazin, J.: Rhythms and community
684 dynamics of a hydrothermal tubeworm assemblage at Main Endeavour Field - A
685 multidisciplinary deep-sea observatory approach, *PLoS One*, 9(5), e96924, 2014.
- 686 Delaney, J. R., Robigou, V., McDuff, R. E. and Tivey, M. K.: Geology of a vigorous
687 hydrothermal system on the Endeavour Segment, Juan de Fuca Ridge, *J. Geophys. Res.*,
688 97(B13), 19663–19682, 1992.
- 689 Van Dover, C. L.: Trophic relationships among invertebrates at the Kairei hydrothermal vent
690 field (Central Indian Ridge), *Mar. Biol.*, 141(4), 761–772, 2002.
- 691 Van Dover, C. L.: Variation in community structure within hydrothermal vent mussel beds of
692 the East Pacific Rise, *Mar. Ecol. Prog. Ser.*, 253, 55–66, 2003.
- 693 Van Dover, C. L. and Fry, B.: Stable isotopic compositions of hydrothermal vent organisms,
694 *Mar. Biol.*, 102(2), 257–263, 1989.
- 695 Van Dover, C. L. and Trask, J. L.: Diversity at deep-sea hydrothermal vent and intertidal
696 mussel beds, *Mar. Ecol. Prog. Ser.*, 195, 169–178, 2000.
- 697 Van Dover, C. L., German, C. R., Speer, K. G., Parson, L. M. and Vrijenhoek, R. C.: Evolution
698 and biogeography of deep-sea vent and seep invertebrates, *Science*, 295(5558), 1253–1257,
699 doi:10.1126/science.1067361, 2002.
- 700 Van Dover, C. and Fry, B.: Microorganisms as food resources at deep-sea hydrothermal
701 vents, *Limnol. Oceanogr.*, 39(1), 51–57, 1994.
- 702 Dreyer, J. C., Knick, K. E., Flickinger, W. B. and Van Dover, C. L.: Development of macrofaunal
703 community structure in mussel beds on the northern East Pacific Rise, *Mar. Ecol. Prog. Ser.*,
704 302, 121–134, 2005.
- 705 Erickson, K. L., Macko, S. A. and Van Dover, C. L.: Evidence for a chemoautotrophically based
706 food web at inactive hydrothermal vents (Manus Basin), *Deep. Res. Part II Top. Stud.*
707 *Oceanogr.*, 56(19–20), 1577–1585, 2009.
- 708 Fisher, C., Takai, K. and Le Bris, N.: Hydrothermal vent ecosystems, *Oceanography*, 20(1), 14–
709 23, 2007.
- 710 Fox, M., Juniper, S. K. and Vali, H.: Chemoautotrophy as a possible nutritional source in the



- 711 hydrothermal vent limpet *Lepetodrilus fucensis*, Cah. Biol. Mar., 43, 371–376, 2002.
- 712 Fretter, V.: New archaeogastropod limpets from hydrothermal vents ; superfamily
713 Lepetodrilacea, Philos. Trans. R. Soc. London, 318, 33–82, 1988.
- 714 Galkin, S. V. and Goroslavskaya, E. I.: Bottom fauna associated with *Bathymodiolus azoricus*
715 (*Mytilidae*) mussel beds in the hydrothermal fields of the Mid-Atlantic Ridge, Oceanology,
716 50(1), 51–60, 2010.
- 717 Gaudron, S. M., Lefebvre, S., Nunes Jorge, A., Gaill, F. and Pradillon, F.: Spatial and temporal
718 variations in food web structure from newly-opened habitat at hydrothermal vents, Mar.
719 Environ. Res., 77, 129–140, 2012.
- 720 Gollner, S., Zekely, J., Dover, C. L. Van, Govenar, B., Le Bris, N., Nemeschkal, H. L., Bright, M.,
721 Hole, W. and Hole, W.: Benthic copepod communities associated with tubeworm and mussel
722 aggregations on the East Pacific Rise, Cah. Biol. Mar., 47(4), 397–402, 2006.
- 723 Govenar, B. and Fisher, C. R.: Experimental evidence of habitat provision by aggregations of
724 *Riftia pachyptila* at hydrothermal vents on the East Pacific Rise, Mar. Ecol., 28(1), 3–14,
725 2007.
- 726 Govenar, B., Le Bris, N., Gollner, S., Glanville, J., Aperghis, A. B., Hourdez, S. and Fisher, C. R.:
727 Epifaunal community structure associated with *Riftia pachyptila* aggregations in chemically
728 different hydrothermal vent habitats, Mar. Ecol. Prog. Ser., 305, 67–77, 2005.
- 729 Govenar, B., Fisher, C. R. and Shank, T. M.: Variation in the diets of hydrothermal vent
730 gastropods, Deep. Res. Part II Top. Stud. Oceanogr., 121, 193–201, 2015.
- 731 Govenar, B. W., Bergquist, D. C., Urcuyo, I. A., Eckner, J. T. and Fisher, C. R.: Three *Ridgeia*
732 *piscesae* assemblages from a single Juan de Fuca Ridge sulphide edifice: Structurally
733 different and functionally similar, Cah. Biol. Mar., 43(3–4), 247–252, 2002.
- 734 Gray, J. S.: The measurement of marine species diversity, with an application to the benthic
735 fauna of the Norwegian continental shelf., J. Exp. Mar. Bio. Ecol., 250(1), 23–49, 2000.
- 736 Grelon, D., Morineaux, M., Desrosiers, G. and Juniper, K.: Feeding and territorial behavior of
737 *Paralvinella sulfincola*, a polychaete worm at deep-sea hydrothermal vents of the Northeast
738 Pacific Ocean, J. Exp. Mar. Bio. Ecol., 329(2), 174–186, 2006.
- 739 Hügler, M. and Sievert, S. M.: Beyond the Calvin cycle: autotrophic carbon fixation in the
740 ocean, Ann. Rev. Mar. Sci., 3, 261–289, 2011.
- 741 Jones, C. G., Lawton, J. H. and Shachak, M.: Organisms as ecosystem engineers, in Ecosystem
742 management, vol. 69, edited by Springer New York, pp. 130–147., 1994.



- 743 Jones, C. G., Lawton, J. H. and Shachak, M.: Positive and negative effects of organisms as
744 physical ecosystem engineers, , 78(7), 1946–1957, 1997.
- 745 Juniper, S. K., Jonasson, I. R., Tunnicliffe, V. and Southward, A. J.: Influence of a tube-building
746 polychaete on hydrothermal chimney mineralization, *Geology*, 20(10), 895–898, 1992.
- 747 Kelley, D. S., Carbotte, S. M., Caress, D. W., Clague, D. A., Delaney, J. R., Gill, J. B., Hadaway,
748 H., Holden, J. F., Hooft, E. E. E., Kellogg, J. P., Lilley, M. D., Stoermer, M., Toomey, D., Weekly,
749 R. and Wilcock, W. S. D.: Endeavour Segment of the Juan de Fuca Ridge: one of the most
750 remarkable places on earth, *Oceanography*, 25(1), 44–61, 2012.
- 751 Kelly, N. E. and Metaxas, A.: Influence of habitat on the reproductive biology of the deep-sea
752 hydrothermal vent limpet *Lepetodrilus fucensis* (Vetigastropoda: Mollusca) from the
753 Northeast Pacific, *Mar. Biol.*, 151(2), 649–662, 2007.
- 754 Lelièvre, Y., Legendre, P., Matabos, M., Mihály, S., Lee, R. W., Sarradin, P.-M., Arango, C. P.
755 and Sarrazin, J.: Astronomical and atmospheric impacts on deep-sea hydrothermal vent
756 invertebrates, *Proc. R. Soc. B Biol. Sci.*, 284(1852), 20162123, 2017.
- 757 Lenihan, H. S., Mills, S. W., Mullineaux, L. S., Peterson, C. H., Fisher, C. R. and Micheli, F.:
758 Biotic interactions at hydrothermal vents: Recruitment inhibition by the mussel
759 *Bathymodiolus thermophilus*, *Deep. Res. Part I Oceanogr. Res. Pap.*, 55(12), 1707–1717,
760 2008.
- 761 Levesque, C., Juniper, S. K. and Marcus, J.: Food resource partitioning and competition
762 among alvinellid polychaetes of Juan de Fuca Ridge hydrothermal vents, *Mar. Ecol. Prog.*
763 *Ser.*, 246, 173–182, 2003.
- 764 Levesque, C., Limén, H. and Juniper, S. K.: Origin, composition and nutritional quality of
765 particulate matter at deep-sea hydrothermal vents on Axial Volcano, NE Pacific, *Mar. Ecol.*
766 *Prog. Ser.*, 289, 43–52, 2005.
- 767 Levesque, C., Kim Juniper, S. and Limén, H.: Spatial organization of food webs along habitat
768 gradients at deep-sea hydrothermal vents on Axial Volcano, Northeast Pacific, *Deep. Res.*
769 *Part I Oceanogr. Res. Pap.*, 53(4), 726–739, 2006.
- 770 Levin, L. A. and Michener, R. H.: Isotopic evidence for chemosynthesis-based nutrition of
771 macrobenthos: the lightness of being at Pacific methane seeps, *Limnol. Oceanogr.*, 47(5),
772 1336–1345, 2002.
- 773 Levin, L. A., Mendoza, G. F., Konotchick, T. and Lee, R.: Macrobenthos community structure
774 and trophic relationships within active and inactive Pacific hydrothermal sediments, *Deep.*



- 775 Res. Part II Top. Stud. Oceanogr., 56(19–20), 1632–1648, 2009.
- 776 Levin, L. A., Ziebis, W., F. Mendoza, G., Bertics, V. J., Washington, T., Gonzalez, J., Thurber, A.
777 R., Ebbe, B. and Lee, R. W.: Ecological release and niche partitioning under stress: Lessons
778 from dorvilleid polychaetes in sulfidic sediments at methane seeps, Deep. Res. Part II Top.
779 Stud. Oceanogr., 92, 214–233, 2013.
- 780 Limén, H., Levesque, C. and Kim Juniper, S.: POM in macro-/meiofaunal food webs
781 associated with three flow regimes at deep-sea hydrothermal vents on Axial Volcano, Juan
782 de Fuca Ridge, Mar. Biol., 153(2), 129–139, 2007.
- 783 Luther, G., Rozan, T., Taillefert, M., Nuzzio, D., Di Meo, C., Shank, T., Lutz, R. and Cary, C.:
784 Chemical speciation drives hydrothermal vent ecology., Nature, 410(6830), 813–816, 2001.
- 785 Marcus, J., Tunnicliffe, V. and Butterfield, D. A.: Post-eruption succession of macrofaunal
786 communities at diffuse flow hydrothermal vents on Axial Volcano, Juan de Fuca Ridge,
787 Northeast Pacific, Deep. Res. Part II Top. Stud. Oceanogr., 56(19–20), 1586–1598, 2009.
- 788 Matabos, M., Le Bris, N., Pendlebury, S. and Thiebaut, E.: Role of physico-chemical
789 environment on gastropod assemblages at hydrothermal vents on the East Pacific Rise (13
790 degrees N/EPR), J. Mar. Biol. Assoc. United Kingdom, 88(5), 995–1008, 2008.
- 791 Matabos, M., Cuvelier, D., Brouard, J., Shillito, B., Ravaux, J., Zbinden, M., Barthelemy, D.,
792 Sarradin, P.-M. and Sarrazin, J.: Behavioural study of two hydrothermal crustacean
793 decapods: *Mirocaris fortunata* and *Segonzacia mesatlantica*, from the lucky strike vent field
794 (mid-Atlantic Ridge), Deep Sea Res. Part II Top. Stud. Oceanogr., 121, 146–158 [online]
795 Available from: <http://linkinghub.elsevier.com/retrieve/pii/S0967064515001113>, 2015.
- 796 McHugh, D. and Tunnicliffe, V.: Ecology and reproductive biology of the hydrothermal vent
797 polychaete *Amphisamytha galapagensis* (Ampharetidae), Mar. Ecol. Prog. Ser., 106, 111–
798 120, 1994.
- 799 Micheli, F., Peterson, C. H., Mullineaux, L. S., Fisher, C. R., Mills, S. W., Sancho, G., Johnson,
800 G. a. and Lenihan, H. S.: Predation structures communities at deep-sea hydrothermal vents,
801 Ecol. Monogr., 72(3), 365–382, 2002.
- 802 Michener, R. and Lajtha, K.: Stable isotopes in ecology and environmental science,
803 Blackwell., 2008.
- 804 Moalic, Y., Desbruyères, D., Duarte, C. M., Rozenfeld, A. F., Bachraty, C. and Arnaud-Haond,
805 S.: Biogeography revisited with network theory: Retracing the history of hydrothermal vent
806 communities, Syst. Biol., 61(1), 127–137, 2011.



- 807 Mullineaux, L. S., Fisher, C. R., Peterson, C. H. and Schaeffer, S. W.: Tubeworm succession at
808 hydrothermal vents: use of biogenic cues to reduce habitat selection error?, *Oecologia*,
809 123(2), 275–284, 2000.
- 810 Mullineaux, L. S., Peterson, C. H., Micheli, F. and Mills, S. W.: Successional mechanism varies
811 along a gradient in hydrothermal fluid flux at deep-sea vents, *Ecol. Monogr.*, 73(4), 523–542,
812 2003.
- 813 Nedoncelle, K., Lartaud, F., de Rafelis, M., Boulila, S. and Le Bris, N.: A new method for high-
814 resolution bivalve growth rate studies in hydrothermal environments, *Mar. Biol.*, 160(6),
815 1427–1439, 2013.
- 816 Nedoncelle, K., Lartaud, F., Contreira-Pereira, L., Yücel, M., Thurnherr, A. M., Mullineaux, L.
817 and Le Bris, N.: *Bathymodiolus* growth dynamics in relation to environmental fluctuations in
818 vent habitats, *Deep Sea Res. Part I Oceanogr. Res. Pap.*, 106, 183–193, 2015.
- 819 Newsome, S. D., del Rio, C. M., Bearhop, S. and Phillips, D. L.: A niche for isotopic ecology,
820 *Front. Ecol. Environ.*, 5(8), 429–436, 2007.
- 821 Oksanen, J., Blanchet, F. G., Friendly, M., Kindt, R., Legendre, P., Mcglinn, D., Minchin, P. R.,
822 O’hara, R. B., Simpson, G. L., Solymos, P., Henry, M., Stevens, H., Szoecs, E. and Wagner, H.:
823 vegan: Community Ecology Package, R Packag. version 2.4-2, [https://CRAN.R-](https://CRAN.R-project.org/package=vegan)
824 [project.org/package=vegan](https://CRAN.R-project.org/package=vegan), 2017.
- 825 Portail, M., Olu, K., Dubois, S. F., Escobar-Briones, E., Gelinis, Y., Menot, L. and Sarrazin, J.:
826 Food-web complexity in Guaymas Basin hydrothermal vents and cold seeps, *PLoS One*, 11(9),
827 e0162263, 2016.
- 828 Ramirez-Llodra, E., Shank, T. and German, C.: Biodiversity and biogeography of hydrothermal
829 vent species: thirty years of discovery and investigations, *Oceanography*, 20(1), 30–41, 2007.
- 830 Sancho, G., Fisher, C. R., Mills, S., Micheli, F., Johnson, G. a., Lenihan, H. S., Peterson, C. H.
831 and Mullineaux, L. S.: Selective predation by the zoarcid fish *Thermarces cerberus* at
832 hydrothermal vents, *Deep. Res. Part I Oceanogr. Res. Pap.*, 52(5), 837–844, 2005.
- 833 Sarrazin, J. and Juniper, S. K.: Biological characteristics of a hydrothermal edifice mosaic
834 community, *Mar. Ecol. Prog. Ser.*, 185, 1–19, 1999.
- 835 Sarrazin, J., Robigou, V., Juniper, S. K. and Delaney, J. R.: Biological and geological dynamics
836 over four years on a high-temperature sulfide structure at the Juan de Fuca Ridge
837 hydrothermal observatory, *Mar. Ecol. Prog. Ser.*, 153(1–3), 5–24, 1997.
- 838 Sarrazin, J., Juniper, S. K., Massoth, G. and Legendre, P.: Physical and chemical factors



- 839 influencing species distributions on hydrothermal sulfide edifices of the Juan de Fuca Ridge,
840 northeast Pacific, *Mar. Ecol. Prog. Ser.*, 190, 89–112, 1999.
- 841 Sarrazin, J., Levesque, C., Juniper, S. K. and Tivey, M. K.: Mosaic community dynamics on
842 Juan de Fuca Ridge sulphide edifices: Substratum, temperature and implications for trophic
843 structure, *Cah. Biol. Mar.*, 43(3–4), 275–279, 2002.
- 844 Sarrazin, J., Cuvelier, D., Peton, L., Legendre, P. and Sarradin, P.-M.: High-resolution
845 dynamics of a deep-sea hydrothermal mussel assemblage monitored by the EMSO-Açores
846 MoMAR observatory, *Deep. Res. Part I Oceanogr. Res. Pap.*, 90(1), 62–75, 2014.
- 847 Sarrazin, J., Legendre, P., de Busserolles, F., Fabri, M. C., Guilini, K., Ivanenko, V. N.,
848 Morineaux, M., Vanreusel, A. and Sarradin, P. M.: Biodiversity patterns, environmental
849 drivers and indicator species on a high-temperature hydrothermal edifice, Mid-Atlantic
850 Ridge, *Deep. Res. Part II Top. Stud. Oceanogr.*, 121, 177–192, 2015.
- 851 Soto, L. A.: Stable carbon and nitrogen isotopic signatures of fauna associated with the deep-
852 sea hydrothermal vent system of Guaymas Basin, Gulf of California, *Deep Sea Res. Part II*
853 *Top. Stud. Oceanogr.*, 56(19–20), 1675–1682, 2009.
- 854 Sweetman, A. K., Levin, L. A., Rapp, H. T. and Schander, C.: Faunal trophic structure at
855 hydrothermal vents on the southern Mohn’s Ridge, Arctic Ocean, *Mar. Ecol. Prog. Ser.*, 473,
856 115–131, 2013.
- 857 Tsurumi, M. and Tunnicliffe, V.: Characteristics of a hydrothermal vent assemblage on a
858 volcanically active segment of Juan de Fuca Ridge, northeast Pacific, *Can. J. Fish. Aquat. Sci.*,
859 58(3), 530–542, 2001.
- 860 Tsurumi, M. and Tunnicliffe, V.: Tubeworm-associated communities at hydrothermal vents
861 on the Juan de Fuca Ridge, northeast Pacific, *Deep. Res. Part I Oceanogr. Res. Pap.*, 50(5),
862 611–629, 2003.
- 863 Tunnicliffe, V.: The biology of hydrothermal vents: ecology and evolution, *Oceanogr. Mar.*
864 *Biol. Annu. Rev.*, 29, 319–407, 1991.
- 865 Turnipseed, M., Knick, K. E., Lipcius, R. N., Dreyer, J. and Van Dover, C. L.: Diversity in mussel
866 beds at deep-sea hydrothermal vents and cold seeps, *Ecol. Lett.*, 6, 518–523, 2003.
- 867 Urcuyo, I., Massoth, G., Julian, D. and Fisher, C.: Habitat, growth and physiological ecology of
868 a basaltic community of *Ridgeia piscesae* from the Juan de Fuca Ridge, *Deep. Res. Part I*
869 *Oceanogr. Res. Pap.*, 50(6), 763–780, 2003.
- 870 Warén, A. and Bouchet, P.: New gastropods from East Pacific hydrothermal vents, *Zool. Scr.*,



871 18(1), 67–102, 1989.
872 Windoffer, R. and Giere, O.: Symbiosis of the hydrothermal vent gastropod *Ifremeria nautilei*
873 (Provannidae) with endobacteria-structural analyses and ecological considerations, Biol.
874 Bull., 193(3), 381–392, 1997.
875 Xu, G., Jackson, D. R., Bemis, K. G. and Rona, P. A.: Time-series measurement of
876 hydrothermal heat flux at the Grotto mound, Endeavour Segment, Juan de Fuca Ridge, Earth
877 Planet. Sci. Lett., 404, 220–231, 2014.
878 Zekely, J., Van Dover, C. L., Nemeschkal, H. L. and Bright, M.: Hydrothermal vent
879 meiobenthos associated with mytilid mussel aggregations from the Mid-Atlantic Ridge and
880 the East Pacific Rise, Deep. Res. Part I Oceanogr. Res. Pap., 53, 1363–1378, 2006.
881
882
883
884
885
886
887
888
889
890
891
892
893
894
895
896
897
898
899
900
901
902

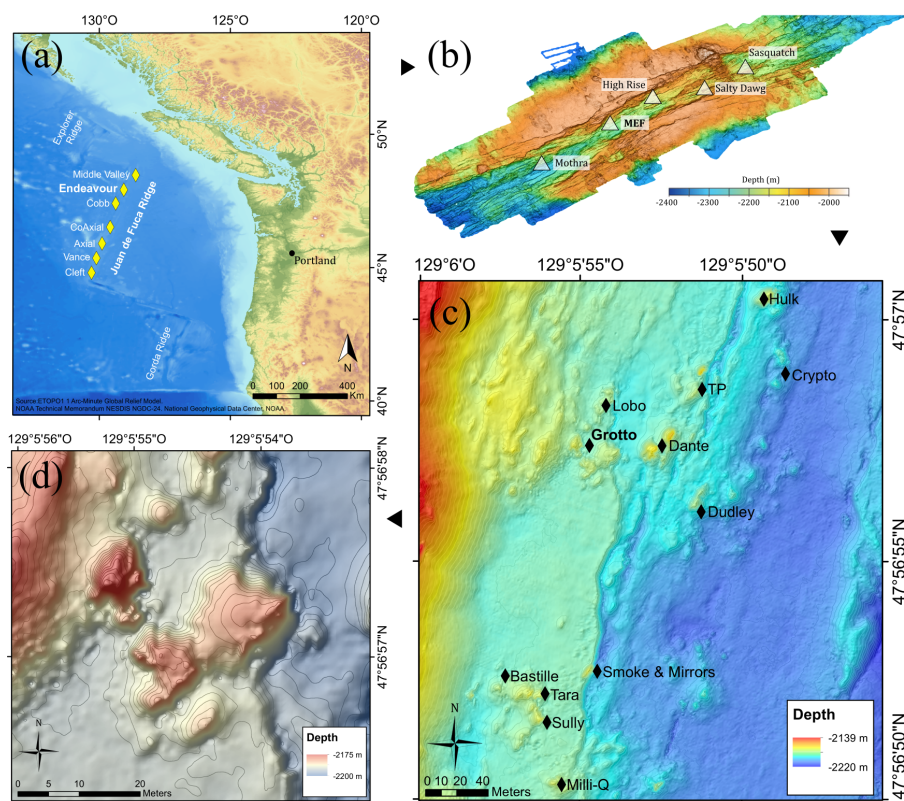


Figure 1. (a) Location of the Juan de Fuca Ridge system and the seven segments (yellow diamonds). (b) High-resolution bathymetric map of the Endeavour Segment, with the locations of the five main active vent fields (white triangle). (c) Location map of the Main Endeavour vent field indicating the positions of hydrothermal vent edifices (black diamonds). (d) Bathymetric map of the Grotto active hydrothermal edifice (47°56.958'N, 129°5.899'W). The 10 m high sulfide structure is located in the Main Endeavour vent field.

903
 904
 905
 906
 907
 908
 909

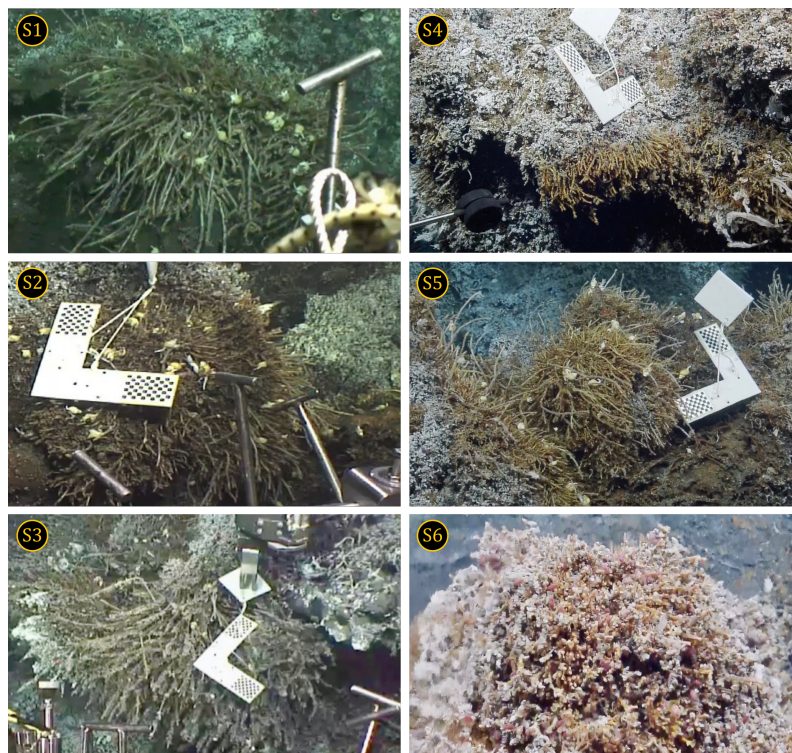


Figure 2. Hydrothermal communities collected on the Grotto edifice (Main Endeavour, Juan de Fuca Ridge) during *Ocean Networks Canada* oceanographic cruises *Wiring the Abyss 2015 and 2016*.

910
911
912
913
914
915
916
917
918
919
920
921
922

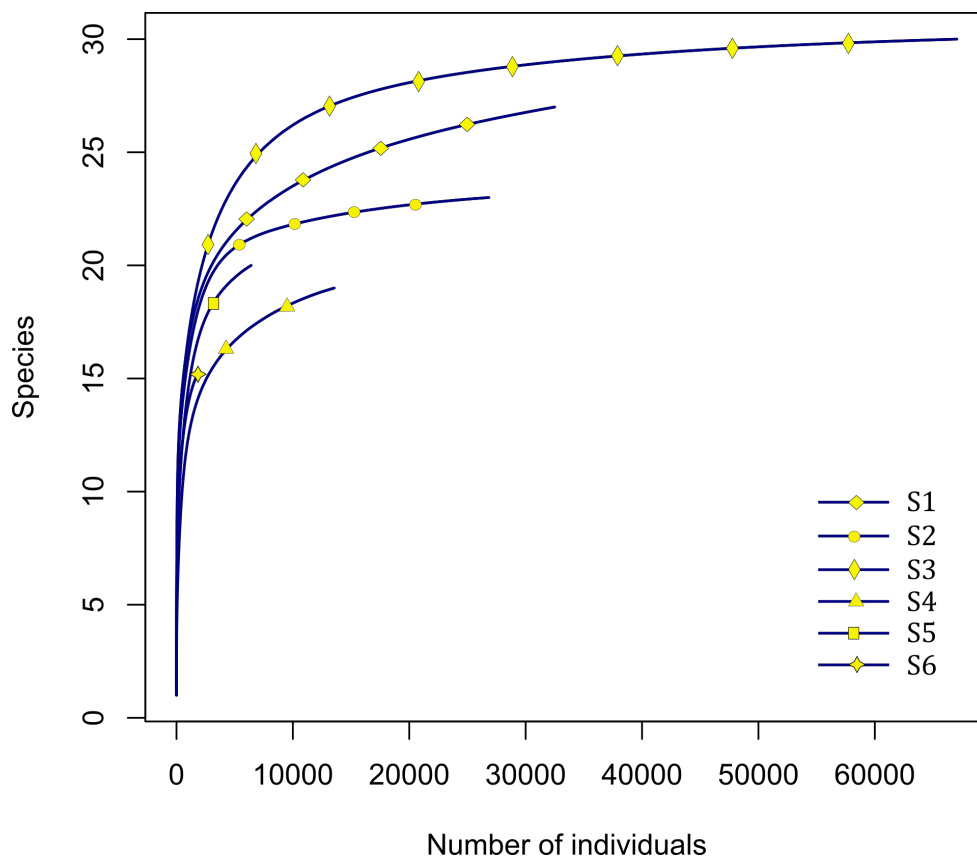


Figure 3. Rarefaction curves for species richness in six vent assemblages (S1 to S6) sampled on the Grotto hydrothermal edifice.

923
924
925
926
927
928
929
930
931
932
933

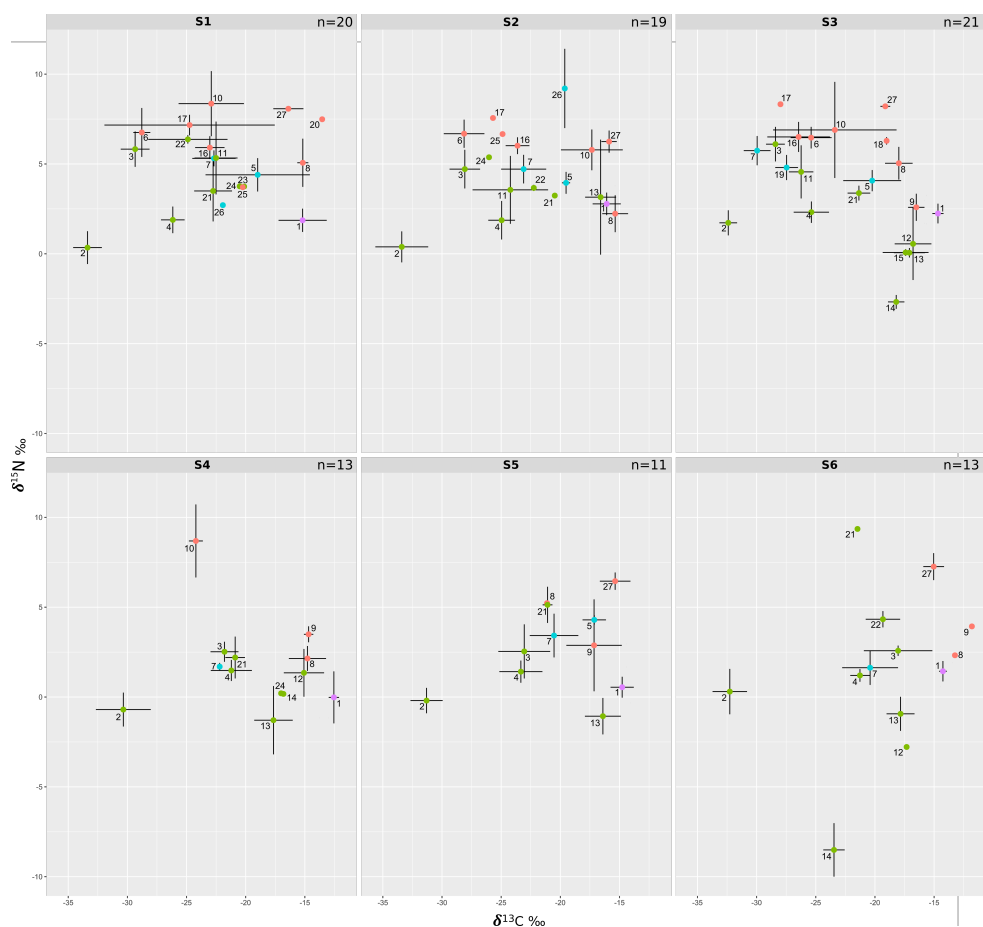


Figure 4. Stable isotope bi-plots showing vent consumers' isotope signatures (mean $\delta^{13}\text{C}$ versus $\delta^{15}\text{N}$ values \pm standard deviation) for the six vent assemblages sampled on the Grotto hydrothermal edifice. Each vent species is designated by a number: 1 = *Ridgeia piscesae*; 2 = *Provanna variabilis*; 3 = *Depressigyra globulus*; 4 = *Lepetodrilus fucensis*; 5 = *Buccinum thermophilum*; 6 = *Clypeosectus curvus*; 7 = *Amphisamytha carldarei*; 8 = *Branchinotogluma tunnicliffeae*; 9 = *Lepidonotopodium piscesae*; 10 = *Levensteiniella kincaidi*; 11 = *Nicomache venticola*; 12 = *Paralvinella sulficola*; 13 = *Paralvinella palmiformis*; 14 = *Paralvinella pandorae*; 15 = *Paralvinella dela*; 16 = *Hesiospina sp. nov.*; 17 = *Sphaerosyllis ridgensis*; 18 = *Ophryotrocha globopalpata*; 19 = *Berkeleyia sp. nov.*; 20 = *Protomystides verenae*; 21 = *Sericosura sp.*; 22 = *Euphilomedes climax*; 23 = *Xylocythere sp. nov.*; 24 = Copepoda; 25 = *Copidognathus papillatus*; 26 = *Paralicella vaporalis*; 27 = *Helicoradomenia juani*. Known trophic guilds are distinguished by a colour code: pink: symbiont; green: bacterivores; blue: scavengers/detritivores; red: predators. For more information on the interpretation of guilds, please consult the web version of this paper.

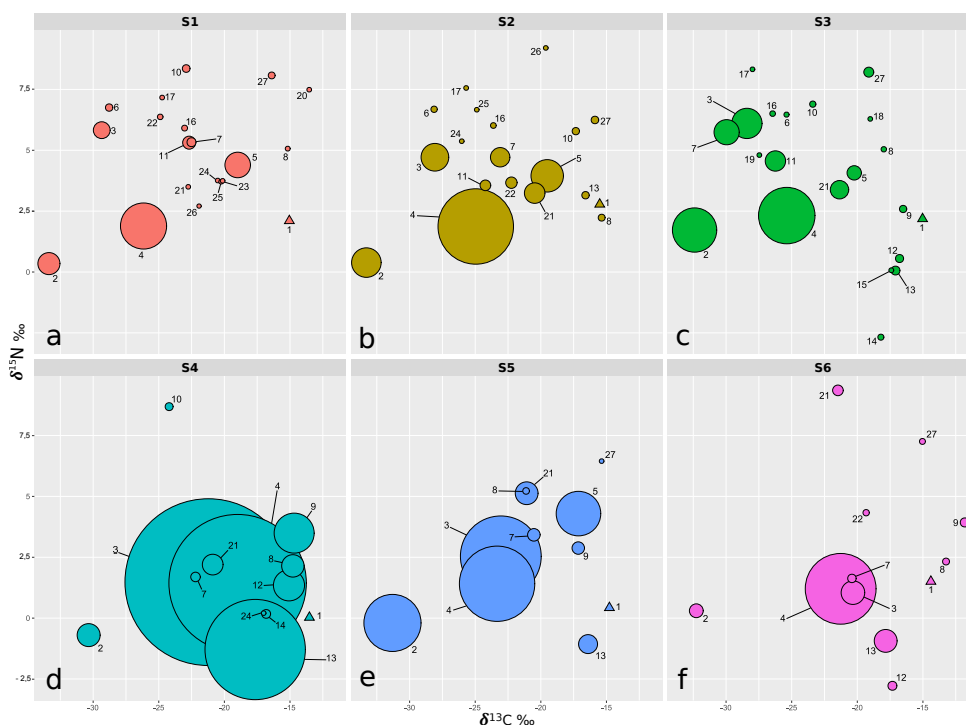


Figure 5. Stable isotope bi-plots showing vent consumers' isotope signatures weighted by biomass per cubic meter (filled circles) for the six vent assemblages (S1 to S6) sampled on the Grotto hydrothermal edifice. Considered as a habitat, the biomass of *Ridgeia piscesae* (denoted by a triangle symbol) is not shown. Each vent species is designated by a number: 1 = *Ridgeia piscesae*; 2 = *Provanna variabilis*; 3 = *Depressigra globulus*; 4 = *Lepetodrilus fucensis*; 5 = *Buccinum thermophilum*; 6 = *Clypeosectus curvus*; 7 = *Amphisamytha carldarei*; 8 = *Branchinotogluma tunnicliffeae*; 9 = *Lepidonotopodium piscesae*; 10 = *Levensteiniella kincaidi*; 11 = *Nicomache venticola*; 12 = *Paralvinella sulfincola*; 13 = *Paralvinella palmiformis*; 14 = *Paralvinella pandorae*; 15 = *Paralvinella dela*; 16 = *Hesiospina sp. nov.*; 17 = *Sphaerosyllis ridgensis*; 18 = *Ophryotrocha globopalpata*; 19 = *Berkeleyia sp. nov.*; 20 = *Protomystides verenae*; 21 = *Sericosura sp.*; 22 = *Euphilomedes climax*; 23 = *Xylocythere sp. nov.*; 24 = Copepoda; 25 = *Copidognathus papillatus*; 26 = *Paralicella vaporalis*; 27 = *Helicoradomenia juani*. For legibility, the biomass of *P. pandorae* in collection S6 is not shown.